A New Detectability Criterion for Conventional Radiography

David TISSEUR [1], Caroline VIENNE [1], Andreas SCHUMM [2], Pierre GUERIN [2],
Philippe DUVAUCHELLE [3], Valérie KAFTANDJIAN [3],
Angela PETERZOL PARMENTIER [4], Uwe EWERT [5]
[1] CEA Saclay DIGITEO Labs, Gif-sur-Yvette, France
[2] EDF R&D, Moret-sur-Loing, France
[3] INSA Lyon, Villeurbanne, France
[4] AREVA NDE Solutions France, Chalon-sur-Saône, France
[5] BAM Bundesanstalt für Materialforschung und -prüfung, Berlin, Germany

Contact e-mail: caroline.vienne@cea.fr

Abstract. For the conventional radiographic technique, X/gamma ray film interpretation is based on human eye perception. There is no criterion of "universal" visibility / detectability of flaws and IQIs for simulated radiography. However, at least one detectability criterion is required for an automatic analysis study of a given set-up. The Rose criterion, based on the contrast to noise ratio of the imaged flaw normalized to the spatial image resolution, is the current reference detectability measure. It is by definition well-adapted in the case of roughly circular flaws (e.g. flat bottom holes or step hole IQIs) but shows its limits for cracks with an elongated shape or close to the limit of spatial resolution as well as for wire IQIs. In this paper, we propose a new detectability criterion to take into account the variability of flaw shape. This paper shows a performance comparison between human expertise and this new criterion, using a large flaw database and IQIs with associated operator evaluations developed in a prior work.

Introduction

In conventional radiographic inspection, a human observer interprets the radiographic image to conclude on the presence of a flaw or the detectability of an image quality indicator (IQI). The problem of characterizing the human ability to detect such a flaw or IQI has been studied since decades, especially through the work of Rose [1], who formulated the human operator ability as a problem of imaging system performance. According to Rose model, detectability of a flaw can be determined by a criterion based on the signal to noise ratio (SNR) measured in the image, where the signal is the contrast between the flaw and its background and the noise is the uncertainty of the measure. Using an experimental approach, Rose defined a perception threshold value around 5 for its criterion, above which human operator is able to detect the signal with significant certainty. Despite the actual limits of Rose model, which have been pointed out by Burgess [2], the notions of detectability criterion and perception threshold are essential in the field of radiographic imaging and more particularly in the context of automatic simulation studies. Indeed, when modelling a radiographic inspection with simulation software, it is

particularly interesting to provide a feedback on the detectability of a given flaw that corresponds to the actual interpretation of human operator reading radiographic film.

In this paper, we use Rose's model as starting point for defining a detectability criterion suitable for conventional radiographic images simulated with CIVA [3] and MODERATO [4] software. This criterion is defined so as to take into account the specificities of the radiographic modelling and the variability of the flaw shape. This paper shows a performance comparison between human expertise and this new criterion, using a large flaw database and IQIs with associated operator evaluations developed in a prior work.

Radiographic Modeling

1.1 Photon-matter interaction

CIVA RT module is used to simulate the results of an inspection carried out with an X-Ray tube or a radioactive gamma ray source. It simulates direct radiation [5] generated by a source and propagating through a specimen, which is defined with potential flaws, and scattering from the specimen in order to create the final radiographic image. The direct radiation is obtained through the analytic Beer-Lambert (BL) law applied along each ray joining the source point to each detector pixel. The scattered radiation is modelled by Monte-Carlo simulation, which computes the path of an individual photon as a random walk, determining both the distance between two interactions (the so called free path length) as well as the type of interaction after having travelled the free path according to random numbers obeying the interaction probability laws. A fusion process is then applied to combine images obtained from these two simulations [6].

1.2 Detector modelling

In the CIVA simulation platform, radiographic film modelling is based on the European standard EN 584 [7] as described in [8]. For conventional radiography, EN584 film modelling is carried out in two successive steps. The first one deals with the calculation of incident dose to the detector and the second one consists in converting the incident dose into signal produced by the complete detection system. This transformation is performed via a transfer function. For EN584 film detector model, this function is pre-computed for each film via a second order equation and allows the generation of optical density (OD) images without noise.

Finally, the film granularity noise is approximated with Gaussian distribution, whose standard deviation σ_D^{simu} is based on the film granularity value (σ_D) available in manufacturers certificates, modified to take into account the pixel size considered in the simulation process:

$$\sigma_D^{simu} = \sigma_D \sqrt{\frac{\pi \cdot 10000}{4A}} \sqrt{\frac{D}{2}}, \qquad (1)$$

where A is the simulation pixel surface in μm² and D is the mean optical density.

1.3 Simulated images

Multiple images can be created during the simulation process for estimating the detectability of a given flaw. They are computed for the object with flaw (complete image displayed to the user) but also for the object without flaw (reference image used for calculation only). These images are detailed here:

- BL direct energy: it corresponds to the deposited energy after a straight line computation on each pixel of the detector. A binary image of the flaw, called flaw mask, is created by first subtracting the BL image of the object with flaw to the BL image of the object without flaw and then thresholding the difference image.
- OD without noise: it corresponds to the simulated radiographic image (including scatter contribution) before application of Gaussian granularity noise. The OD images without noise are computed with the flaw (resp. without it) and convoluted with the flaw mask to compute the mean value of OD of the flaw (resp. of the background).
- OD with noise: it corresponds to the final image (including scatter contribution) simulating the real radiographic image.

2. Detectability criterion

Based on the Rose model, we propose here a detectability criterion that depends on the signal value, on the noise level and on the flaw surface. We detail the computation of these different parameters for ensuring a good performance of the criterion.

2.1 Signal intensity

In the context of flaw detection, the signal corresponds to image contrast, defined as intensity change between the flaw and its neighbourhood. To compute this value in the CIVA environment, we can use OD images without noise simulated with and without flaw, as detailed in the previous section. The knowledge of the flaw mask, computed from BL images allows the computation of contrast C from mean OD values of the flaw OD_{flaw} and its background OD_{bg}:

$$C = \left\| OD_{flaw} - OD_{bg} \right\|$$

2.2 Noise level

According to detector modelling implemented in the CIVA software, the noise level measured in the artificial image σ_D^{simu} is dependent on the pixel size used in the simulation process. In practice, this pixel size does not account for a real radiographic acquisition parameter and should not influence the noise level considered in the detectability criterion.
To free ourselves from simulation parameters and model the human operator ability, we express equation (1) in the case of a pixel size corresponding to eye resolution. The noise value is then:

$$\sigma_D^{eye} = \sigma_D^{simu} \frac{pixel\_size}{eye\_resolution}$$

According to [9], we can consider that a human eye with an optimal acuity presents a resolution equal to 1 arc min. If we consider an eye to radiographic film distance equal to 40 cm, the eye resolution is around 120 μm.

2.3 Considered flaw surface

One modification is brought to the Rose detectability criterion to expand the initial criterion, established for circular shapes (see **Fig. 1**), to the case of elongated shapes.
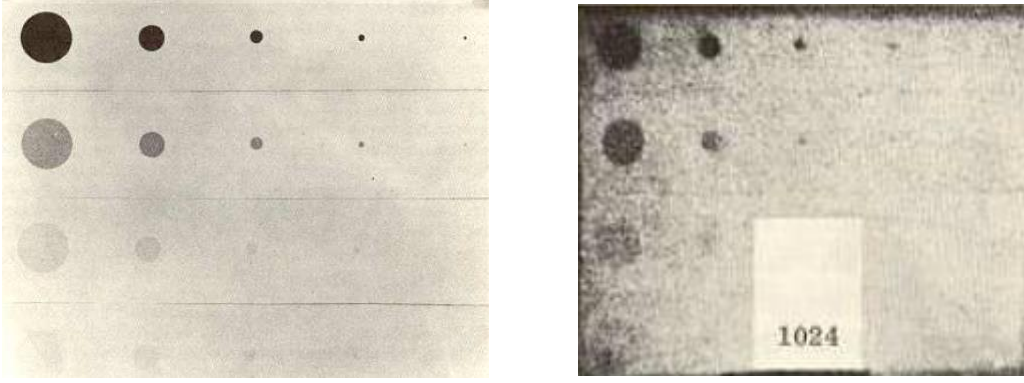
Fig. 1: Test pattern (left) and resulting image (right) used by Rose in [1] to establish its theory.

This modification is based on the knowledge that there is no direct equivalence between the visibility of step hole IQI and wire IQI. More particularly, by referring to French code "Design and Construction Rules for the Mechanical Components of PWR Nuclear Islands" (RCCM) [10], we can determine that step hole IQI of diameter $\emptyset$ has a visibility equivalent to wire IQI of diameter $\emptyset/2.5$ (see **Fig. 2**). Similar work has been previously done for digital radiography and shows a nonlinear relationship between wire and hole diameters [11].
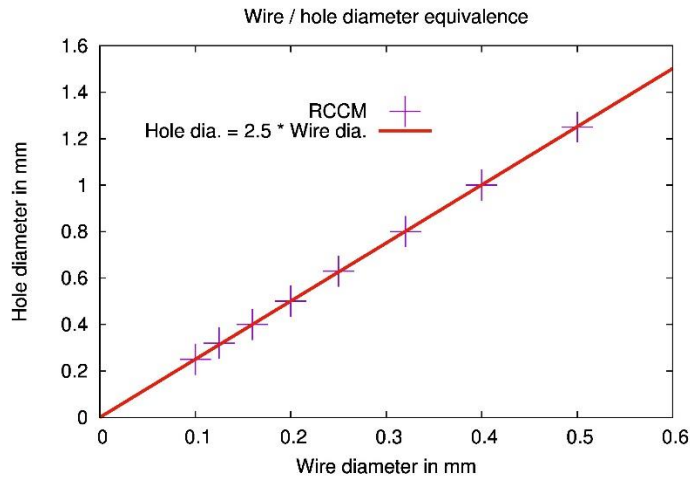

Fig. 2: Wire/hole equivalence using French radiographic code RCCM

Due to this observation, we propose to estimate, in the case of elongated shapes, the surface S_{eq} of a circular shape of equivalent visibility.

After extracting the mask of the flaw with BL images, we perform a Principal Component Analysis (PCA) to compute the eigenvalues λ_1, λ_2 of the flaw shape, which are proportional to the squared length of eigenvectors. The eccentricity of the flaw is then computed as:

$$\varepsilon = \sqrt{1 - \frac{\lambda_2}{\lambda_1}}.$$

If this eccentricity is below the value $\varepsilon_{th} = 0.87$ corresponding to a shape ratio of 2, then the flaw is considered as circular and fits in Rose model. Otherwise, it is considered as a wire and the diameter of equivalent hole $\emptyset = 2.5B$, where B is the small axis of the flaw (see **Fig. 3**), is used to compute the equivalent object surface:

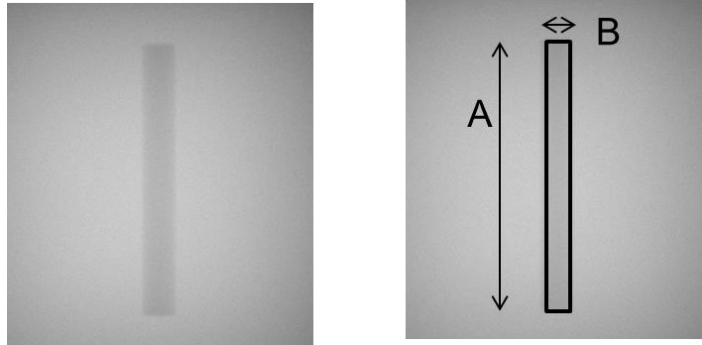$$S_{eq} = \frac{\emptyset^2}{4} \cdot \pi$$

4

Fig. 3: Flaw eccentricity is estimated from PCA and for elongated shapes the small axis length B is considered for surface computation.

Finally a threshold is applied to this surface value so as to model the fact that above a size of 1.6 mm², a larger surface of the flaw does not imply a better detectability of the flaw:

$$S = \min(S_{eq}, 1.6).$$

2.4 Implemented criterion

The proposed formula for flaw detectability in simulated conventional radiographic images is therefore:

$$Criterion = \frac{C}{\sigma_D^{eye}} \cdot \sqrt{S}$$

3. Simulation of radiographic inspection

3.1 Case 1

First radiographic trials have been realized with an Ir192 source and C2 Kodak M100 film on mock-ups of artificial cylindrical flaws (see **Fig. 4**). Flaws have 10 mm diameter and various depths between 98 μm and 695 μm. Different control configurations have been considered with variation on pipe thickness (a), source distance (b) and number of crossed pipe walls.
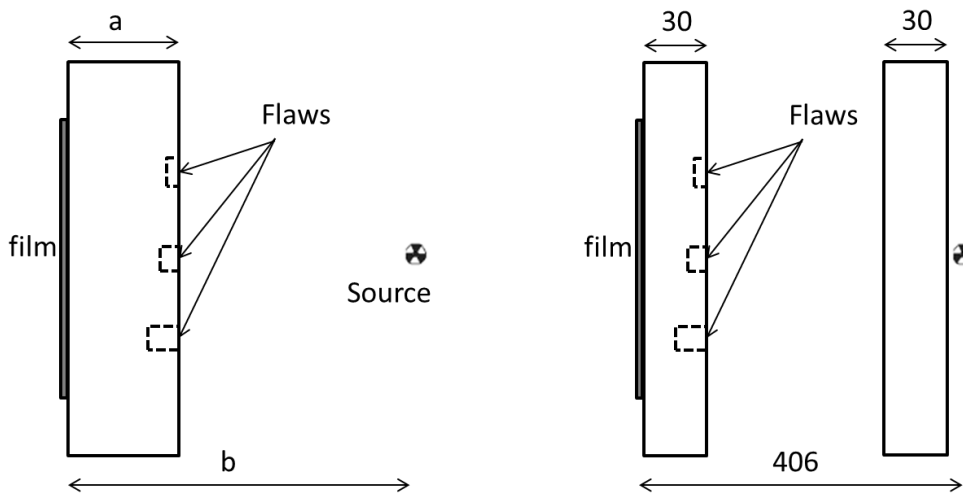

Fig. 4: First case study involves two simple wall configurations (left), with a = 92 mm and b = 390 mm (respectively a = 56 mm and b = 421 mm) and one double wall configuration (right).

Case 1 has been simulated with MODERATO by using a pixel size of 20 μm. Examples of OD simulated images are displayed in **Fig. 5**.
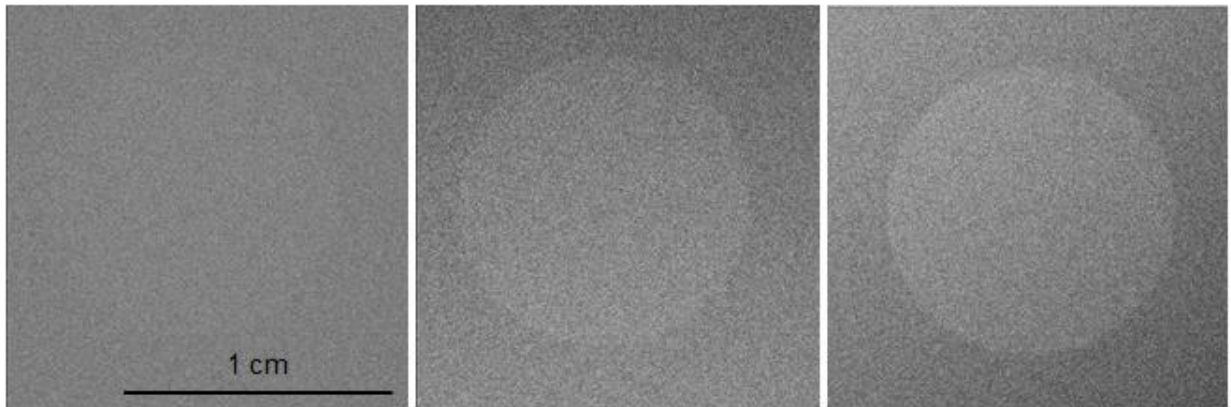
Fig. 5: Simulated images from double walls acquisition with different flaw depths.

Radiographic images coming from real acquisition are interpreted by human operators who classify them into three categories:
- flaw not seen (0)
- flaw seen with uncertainty (detectability limit = 1)
- flaw seen (2)

3.2 Case 2

The second case study consists in artificial flaws created from parts of IQI of steel and copper and from wires of lead and tungsten. 192 flaws are put on the inner wall of a steel plate of 51 mm thickness and 30 cm x 30 cm size (see **Fig. 6**). The experimental set-up is constituted of a fixed frame on which the mock-up of 192 flaws and one Ir192 source are fixed. A C2 Kodak M100 film is placed upon contact with the mock up and is interpreted by three experts. Each flaw has been noted between from 0 (no seen) to 5 (clearly seen). For each flaw, we take into account the mean evaluation from the three experts.
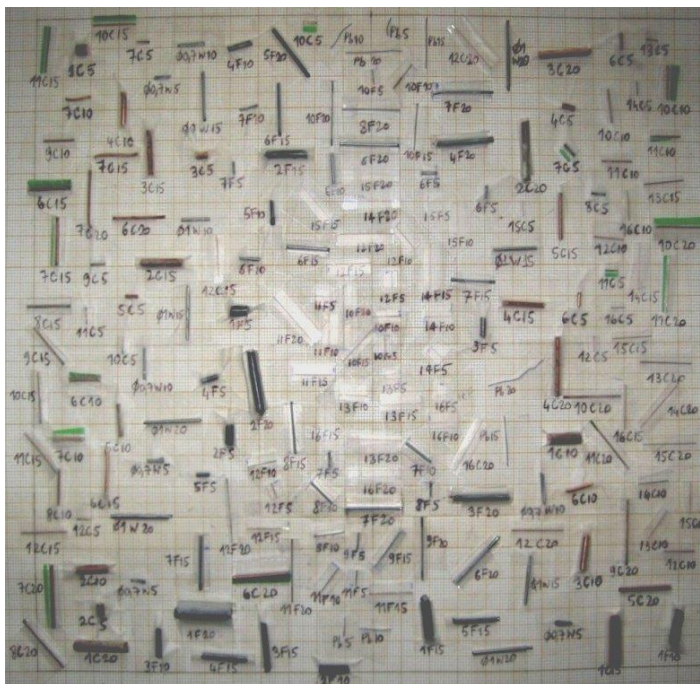
➢ Fe, Cu: Ø 0,05 à 3,2 mm, L = 5, 10, 15, 20 mm

➢ Pb: Ø 0,25 mm, L = 5, 10, 15, 20 mm

➢ W: Ø 0,7 et 1 mm, L = 5, 10, 15, 20 mm

Fig. 6: Mock-up of 192 flaws created from IQI parts and wires used in the second case study.

This configuration is simulated with CIVA by using a pixel size of 20 µm. Two samples of OD images are displayed in **Fig. 7**. They correspond to one copper IQI of small diameter declared "not seen" by operators (on left) and one copper IQI of large diameter declared "seen" (on right).
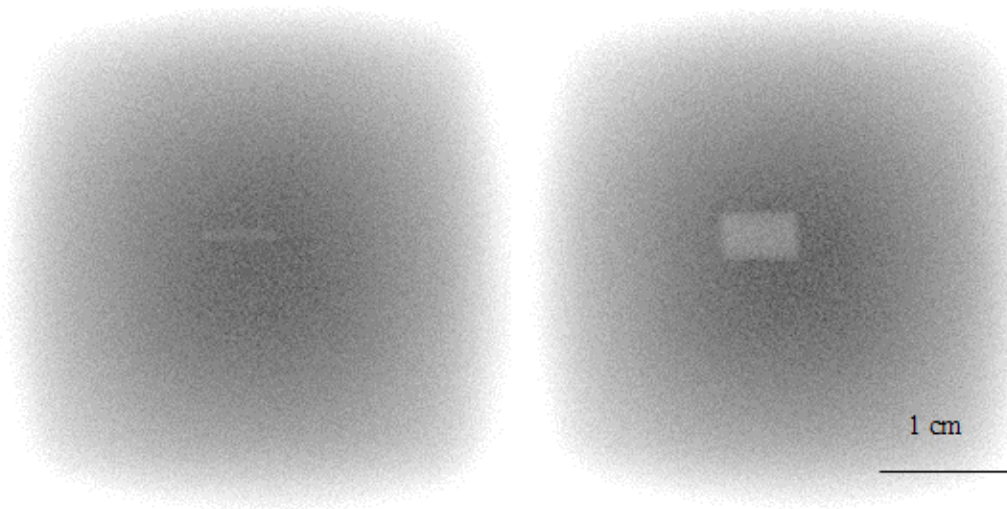

Fig. 7: Simulated images of copper flaws of diameter 0.8 mm (left) and 3.2 mm (right).

4. Performance of the criterion

The following figure presents a synthetic view of the performance of the criterion versus expert notation. With this graph, we can separate the results in 4 domains:
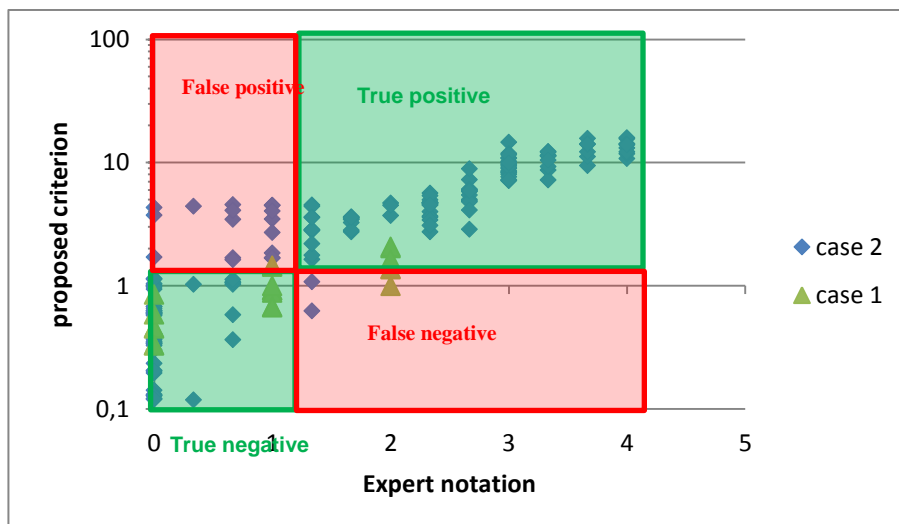- true positive
- true negative
- false positive
- false negative

Fig. 8: Synthetic view of the performance of the criterion results versus expert notation

With the new proposed criterion, a detectability threshold of 1.5 resulted the most suited in determining the detectability of the defects, independently of their shape and of the pixel size of the simulation. With this threshold value, we found an agreement between the

criterion and the experts evaluation for 190 flaws for a total of 202 tested flaws (20 flaws for case 1 and 192 flaws for case 2).

5. Conclusion

The proposed detectability criterion shows good performances with respect to experts evaluations obtained through two case studies. By taking into account simulations performed with MODERATO and CIVA, a compromise between an "optimistic" criterion and a "pessimistic" one seems to show that it is necessary to use a detectability threshold of 1.5. With this value, we found an agreement between expert judgment and the criterion for 89.6 % of the flaws over 202 flaws tested. This new criterion will be available in CIVA and MODERATO in 2016. Further work will include case studies with background gradient and cracks type flaws.

References

[1] A. Rose, Vision: human and electronic, New York, NY: Plenum, 1973.

[2] A. E. Burgess, "The Rose model, revisited," *Journal of the Optical Society of America A: Optics, Image Science, and Vision,* pp. Volume 16, Issue 3, pp.633-646, 1999.

[3] CIVA, "http://www-civa.cea.fr," [Online].

[4] A. Bonin, B. Lavayssière et B. Chalmond, «"MODERATO: a Monte-Carlo Radiographic Simulation",,» *Proc. Review of Progress in Quantitative NDE, QNDE 99,* 1999.

[5] R. Fernandez, A. Schumm, J. Tabary and P. Hugonnard, "Simulation studies of radiographic inspections," in *WCNDT*, Shanghai, China, 2008.

[6] J. Tabary, R. Guillemaud, F. Mathy, A. Gliére et P. Hugonnard, «Combination of high resolution analytically computed uncollided flux images with low resolution Monte-Carlo computed scattered flux images,» *IEEE Transaction on nuclear science,* vol. 51, n° %11, pp. 212-217, 2004.

[7] E. 584-1:2006, "Non-destructive testing – Industrial radiographic film – Part 1: Classification of film systems for industrial radiography," in *European standard for non-destructive evaluation*.

[8] A. Schumm and U. Zscherpel, "The EN584 Standard for the Classification of Industrial Radiography Films and its Use in Radiographic Modelling," in *6th International Conference on NDE in Relation to Structural Integrity for Nuclear and Pressurized Components*, Budapest, Hungary, 2007.

[9] M. Schraufa et C. Stern, «The visual resolution of Landolt-C optotypes in human subjects depends on their orientation: the gap-down effect,» *Neuroscience Letters,* 2001.

[10] AFCEN, Design and Construction Rules for Mechanical Components of PWR Nuclear Islands RCC-M, Addendum : AFCEN, 1985.

[11] U. Ewert, U. Zscherpel, K. Heyne, M. Jechow and K. Bavendiek, "Image Quality in Digital Industrial Radiography," *Material Evaluation,* vol. 70, no. 8, pp. 955-964, 2012.